

Communication

A Wideband Circularly Polarized Magnetolectric Dipole Antenna for 5G Millimeter-Wave Communications

Hussain Askari ^{1,†} , Niamat Hussain ^{2,†} , Md. Abu Sufian ¹, Sang Min Lee ³ and Nam Kim ^{1,*}

¹ Department of Information and Communication, Chungbuk National University, Cheongju 28644, Korea; askarihussain01@gmail.com (H.A.); abu.sufian@chungbuk.ac.kr (M.A.S.)

² Department of Smart Device Engineering, Sejong University, Seoul 05006, Korea; niamathussain@sejong.ac.kr

³ Department of Corporate Support Centre, Korea National University of Transportation, Chungju-si 27469, Korea; leesm@ut.ac.kr

* Correspondence: namkim@chungbuk.ac.kr

† These authors contributed equally to this work.

Abstract: In this paper, a wideband circularly polarized (CP) magnetolectric (ME) dipole antenna operating at 28 GHz band was proposed for 5G millimeter-wave (mm-wave) communications. The antenna geometry included two metallic plates with extended hook-shaped strips at its principal diagonal position, and two corners of truncated metallic plates at the secondary diagonal position. The pair of metallic vias connected the modified strips to the ground plane to create the magnetic dipole. The L-shaped probe feed between the strips was used to excite the antenna. The antenna showed stable gain and wideband characteristics. The simulated and measured results showed that the proposed CP ME dipole antenna had an overlapping ($|S_{11}| < -10$ dB impedance and 3 dB axial ratio) bandwidth of 18.1% (25–30 GHz), covering the frequency bands dedicated for 5G new radio communications. Moreover, an average gain of 8 dBic was achieved by the antenna throughout the operating bandwidth. The measured data verified the design concept, and the proposed antenna had a small footprint of $0.83 \lambda_0 \times 0.83 \lambda_0 \times 0.125 \lambda_0$ (λ_0 is free space wavelength at the lowest operating frequency), suitable for its application in 5G smart devices and sensors.

Keywords: magnetolectric; dipole; circularly polarized; 5G antenna; 28 GHz



Citation: Askari, H.; Hussain, N.; Sufian, M.A.; Lee, S.M.; Kim, N. A Wideband Circularly Polarized Magnetolectric Dipole Antenna for 5G Millimeter-Wave Communications. *Sensors* **2022**, *22*, 2338. <https://doi.org/10.3390/s22062338>

Academic Editors: Raed A. Abd-Alhameed, Chan Hwang See and Naser Ojaroudi Parchin

Received: 16 February 2022

Accepted: 16 March 2022

Published: 17 March 2022

Publisher's Note: MDPI stays neutral with regard to jurisdictional claims in published maps and institutional affiliations.



Copyright: © 2022 by the authors. Licensee MDPI, Basel, Switzerland. This article is an open access article distributed under the terms and conditions of the Creative Commons Attribution (CC BY) license (<https://creativecommons.org/licenses/by/4.0/>).

1. Introduction

The twenty-first century has experienced tremendous development in the field of wireless communication. The fast evolving fifth-generation (5G) technology has brought new advancements which have posed a great challenge for antenna researchers and engineers. Large channel capacity and high data rates should be achieved to meet the demands of the 5G communication link. In this scenario, the millimeter-wave (mm-wave) band is used to fulfill the gigabit high-data transmission, and addresses the lack of wider spectral resource in the currently allocated band below 6 GHz [1]. Recently, the third-generation partnership project (3GPP) has allocated new radio (NR) frequency bands in the mm-wave range from 24.25 to 29.5 GHz, which are known as n257 and n258. Figure 1 shows the mm-wave frequency band distribution adopted by the leading 5G countries in the world [2].

In addition, circularly polarized (CP) antennas have been a unique choice for stable communication due to their resilience to multipath interference and polarization mismatching between receiving and transmitting antennas. These features make CP antennas the desirable candidate for numerous applications including satellite communication, radar communication, randomly oriented RFID (radio frequency identification) tags, GPS (global positioning system), and sensors [3–9]. Therefore, the design of CP antennas has always been a hot topic for antenna designers, compared with linear polarized (LP) antennas. In the literature, different kinds of CP antennas have been reported for mm-wave applications,

including patch antenna, aperture antenna, slot antenna, cavity antenna, and magneto-electric (ME) dipole antenna. The ME dipole antenna is the most popular type of antenna due to its complementary performance.

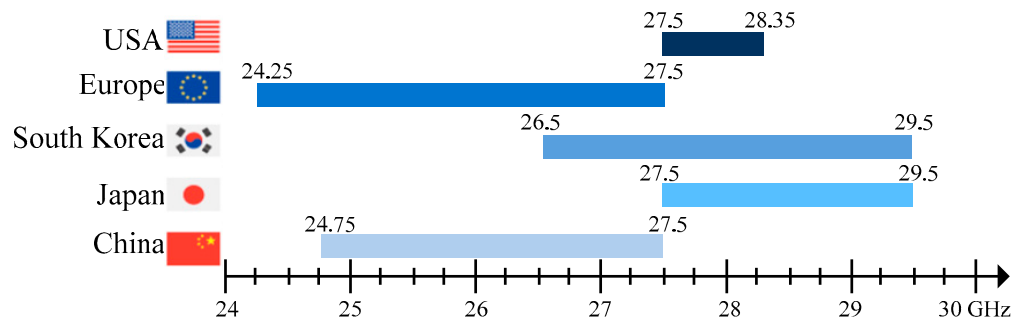


Figure 1. Global snapshot of the 5G millimeter-wave spectrum.

The concept of the first ever complimentary antenna was proposed by Chlavin in 1954 [10]. Since then, many structures were proposed based on a slot/dipole or a slot/monopole combination. In 2006, Luk and Wong introduced a complementary antenna based on patch and dipole antenna combinations for the first time, achieving wideband performance [11]. The idea used a pair of copper patches parallel to the ground as an electric dipole and a pair of copper shorted patches perpendicular to the ground as a magnetic dipole. The antenna showed linear polarization with wide bandwidth, stable gain, and low levels of cross-polarization. In the course of designing ME dipole antennas [12,13], less attention has been paid to CP ME dipole based antennas. In the past few years, some CP antennas based on ME dipole structures have been reported [8,14–21]. In [14], an ME dipole structure was reported to use a pair of bowtie patch antennas and a pair of trapezoidal-shaped dipoles fed by a Wilkinson power divider to achieve a 3 dB AR bandwidth of 33%. Moreover, to ensure the CP radiation was presented, an ME dipole antenna was integrated with a crossed dipole fed by double phased delay rings in [15]. The proposed antenna achieved 27.67% of 3 dB AR bandwidth. In [16], substrate integrated waveguide (SIW) and aperture coupled feeding was used to excite an ME dipole antenna for mm-wave applications. This antenna achieved a 3 dB AR bandwidth of 12.8%. However, the above-mentioned reported ME dipole antennas showed limited AR bandwidth and had complex feeding structures. The wideband ME dipole antennas investigated in [17,18] had the advantage of a wider 3 dB AR bandwidth of 71.5% and 47.7%, respectively. However, the drawback of these antennas was their huge volume which limits their usage in modern electronic devices and sensors. On the other hand, the CP ME antennas designed at 60 GHz band offer wide AR bandwidth/high gain at the expense of large antenna size [19–21]. In [22], the AR bandwidth of the ME dipole antenna was significantly improved (53%) by employing a novel crossed feeding structure. This design has a high antenna profile (33.3 mm antenna height) and limited gain (6.6 dBic). A wideband circularly polarized ME dipole array fed by a complementary SIW power distribution phase shifter was presented [23]. The single-element antenna gain was 7dBic, while the AR bandwidth was restricted to 9.7%. To mitigate increased atmospheric losses in mm-wave bands, the gain of the wideband CP ME dipole antennas was increased in [24,25]. Moreover, the ME dipole antenna offered the advantages of low-profile and wide bandwidth with LP radiation [26]. In summary, the existing CP ME dipole antennas are suffering from either narrowband operation or high antenna profiles.

In this paper, a compact, wideband CP ME antenna operating at 28 GHz band is presented for 5G communications. The antenna's CP bandwidth covers 25–30 GHz band (18.1%), covering the frequency bands dedicated for 5G new radio communications. Moreover, the antenna offers stable gain (average 8 dBic) and radiation patterns, with the advantages of a small footprint ($0.9 \lambda_0 \times 0.9 \lambda_0 \times 0.14 \lambda_0$) for its applications in 5G smart devices and sensors.

The rest of the manuscript has been structured as follows: Section 2 explains the detailed analysis and design of the proposed circularly polarized ME dipole antenna. The simulated and measured results have been presented in Section 3, while the paper has been concluded in Section 4.

2. CP ME Antenna Design and Analysis

2.1. Antenna Geometry

The schematics of the proposed CP ME dipole antenna are shown in Figure 2. The antenna is composed of two metallic strips with an extended hook shape on its principal diagonal position, two L-shaped metallic strips on secondary diagonal position, and four sets of via holes. The modified metallic strips above the ground plane act as two planar electric dipoles. The four sets of via holes, each containing three metallic plated vias, are shorted between the modified patches and the ground plane. The metallic vias and the ground plane between them act as a magnetic dipole. The antenna is fed by an L-shaped probe to achieve low cross-polarization and back radiation levels [27,28]. The metallic patch of L-shaped probe acts as a coplanar waveguide (CPW) feed between the planar dipoles, which work as coplanar grounds. A square size (10 mm × 10 mm) Rogers 5880 with a thickness of 1.5 mm was used as the substrate of the antenna. The proposed ME dipole antenna’s optimized dimensions are summarized in Table 1.

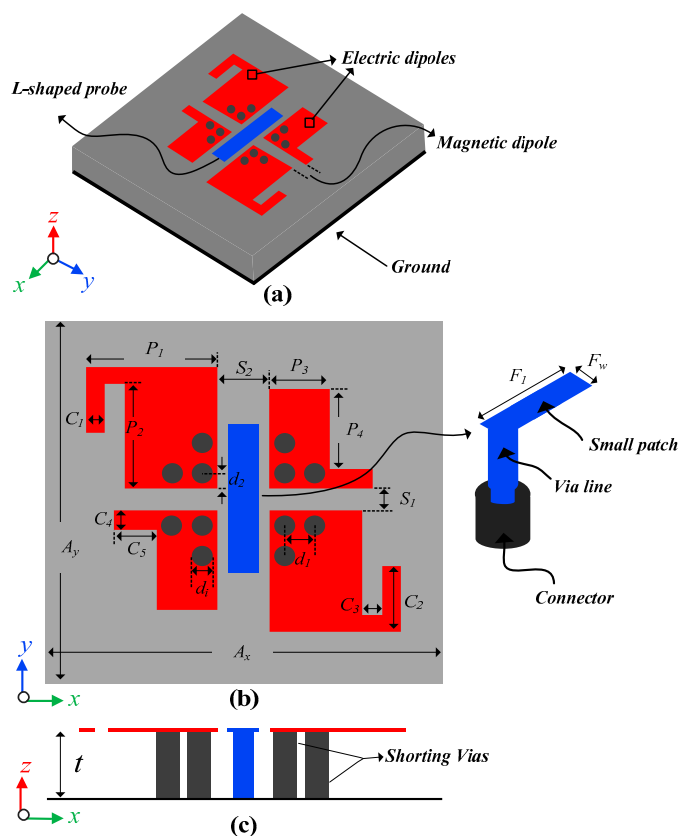


Figure 2. The geometry of the proposed CP ME antenna: (a) 3D view, (b) top view, and (c) side view.

Table 1. Optimized dimensions of the proposed CP ME dipole antenna.

Parameter	Value (mm)	Parameter	Value (mm)	Parameter	Value (mm)
t	1.5	P_4	1.8	C_4	0.45
F_1	2.5	S_1	0.5	C_5	1
F_w	0.7	S_2	1	d_i	0.5
P_1	3	C_1	0.4	d_1	0.7
P_2	2.4	C_2	1.5	d_2	0.35
P_3	1.4	C_3	0.5	A_x, A_y	10

During the antenna design, we found that the antenna offered optimum performance under the given constraints of the optimized parameters. Changing any parameter may disturb the AR or impedance bandwidth, or even both. In particular, varying the length of the patch (F_1) changed the $|S_{11}|$ resonance of the antenna, however, the AR resonance did not change significantly. The distance between the monopole and metallic strips (S_2) and S_1 was sensitive to both $|S_{11}|$ and AR bandwidth. A small change may deteriorate the overlapping bandwidth. Similarly, all other parameters, especially S_1 , C_1 , C_2 , C_3 , C_4 , and C_5 should be carefully tuned to achieve the best possible usable bandwidth.

2.2. CP Mechanism

The CP mechanism of the proposed ME dipole antenna can easily be understood by visualizing the surface current distributions on coplanar electric dipoles, as shown in Figure 3. The surface current distributions were examined and recorded at 28 GHz for different time phases of 0° , 90° , 180° , and 270° . It can be noticed that the vector representation of surface current rotates in an anti-clockwise direction as the phase shifts from 0° to 90° , 180° , and 270° . The resultant vector of these surface current distributions makes a quasi-loop due to the rotational symmetry of this antenna, a necessary condition for CP radiation [29–31]. Thus, the proposed ME dipole antenna generates right-hand circular polarization (RHCP) in the positive z -axis direction.

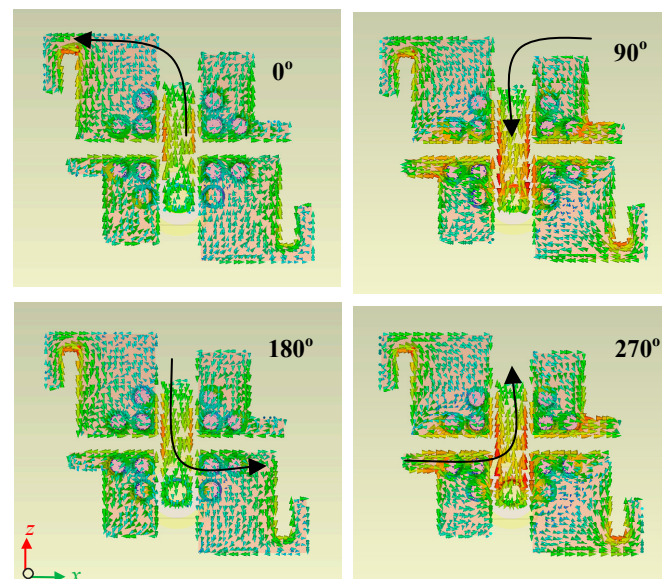


Figure 3. Surface current distributions of the proposed CP ME dipole antenna for different time phases at 28 GHz.

The origin of CP radiations in the antenna is further explained by considering the degenerated modes which are excited in the planar electric dipoles and L-shaped microstrip patch antenna, separately. At time $t = 0$, the aperture of the shorted L-shaped patch acquires maximum surface current, and similarly for the time $t = T/2$, but at this latter time, the direction of surface current is opposite. Therefore, this causes induction of equivalent and

orthogonal magnetic current in the aperture of the same L-shaped patch along the x -axis, which causes a 90 degree phase difference with respect to electric surface currents. In time $t = T/4$ and $3T/4$, the planar electric dipoles attain maximum and opposite directed electric surface currents at their edges. It can be noted that the direction of electric surface currents on planar dipoles is also along the x -axis. Hence, the equivalent electric and magnetic currents are directed in the same direction and are in phase. This is how the proposed antenna can generate the CP radiation.

3. Results and Discussion

The proposed CP ME dipole antenna's prototype was fabricated and measured to verify its performance, as shown in Figure 4. Figure 4a shows the fabricated prototype of the proposed antenna. The setup for the antenna far field measurements is illustrated in Figure 4b. The antenna was measured in a multi-probe 360 degree scanning anechoic chamber. Overall, the simulated results showed good agreement with the measured results.

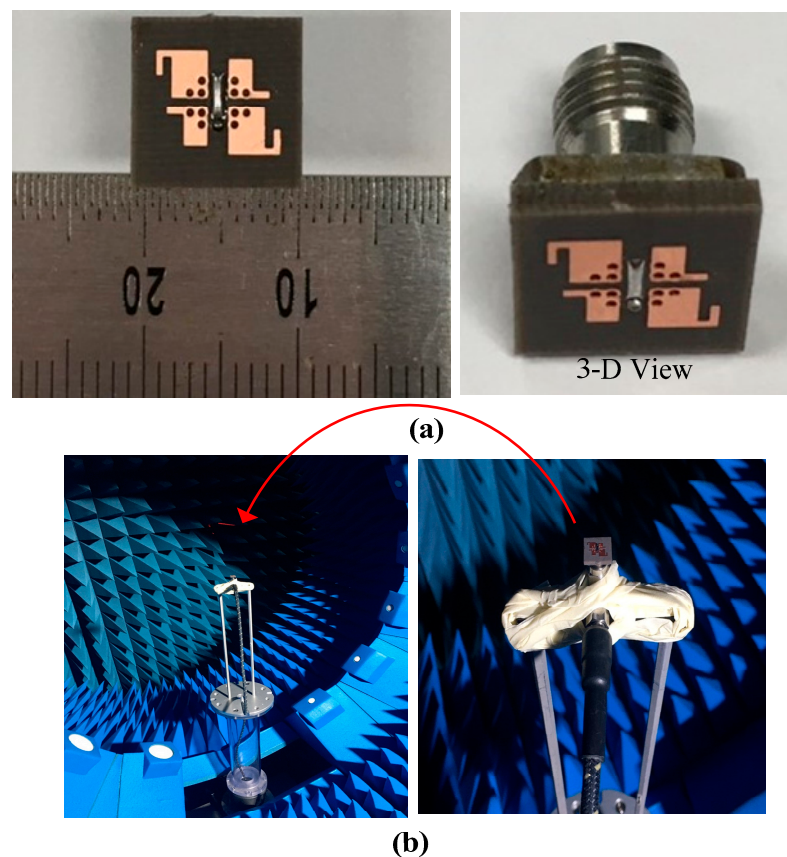


Figure 4. Photographs of the proposed CP ME dipole antenna: (a) fabricated prototype and (b) far field measurement setup.

3.1. S-Parameters and Axial Ratio

The measurement result for the S-parameter $|S_{11}|$ was obtained using a network analyzer (Rohde and Schwarz ZVA 40) in open air condition. The little difference in simulated and measured results, as shown in Figure 5a, was due to connector/cable losses. The proposed antenna has an impedance bandwidth for $|S_{11}| < -10$ dB was 24.6%, that is, from 24.1 to 31.0 GHz. The simulated and measured 3 dB AR bandwidth of the proposed antenna was 18.1%, ranging from 25 to 30 GHz, as shown in Figure 5b. Thus, the overlapping operating bandwidth of the antenna covered the important band spectrum proposed for 5G mm-wave applications.

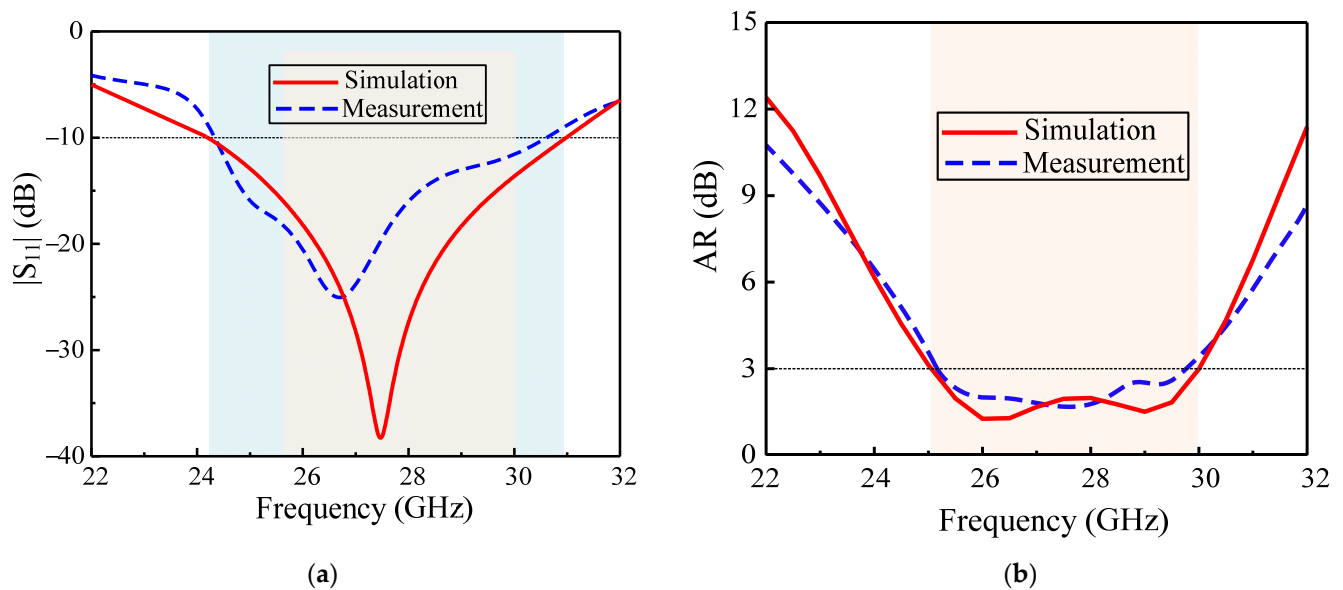


Figure 5. Proposed CP ME dipole antenna: (a) S-parameter $|S_{11}|$ and (b) axial ratio.

3.2. Broadside Gain and Efficiency

The simulated and measured broadside gain of the proposed antenna is shown in Figure 6a. The antenna showed a stable broadside gain of 8 dBic with a deviation of only ± 0.5 dBic within the frequency range of interest. Moreover, the antenna also offered high efficiency, both total and radiation efficiency, due to good antenna impedance matching (Figure 6b). The simulated radiation efficiency of the antenna was more than 96%, which was in close agreement with its measured value. The measured total efficiency was observed to be a little lower than its simulated values (88%) due to possible cable/connector and substrate losses.

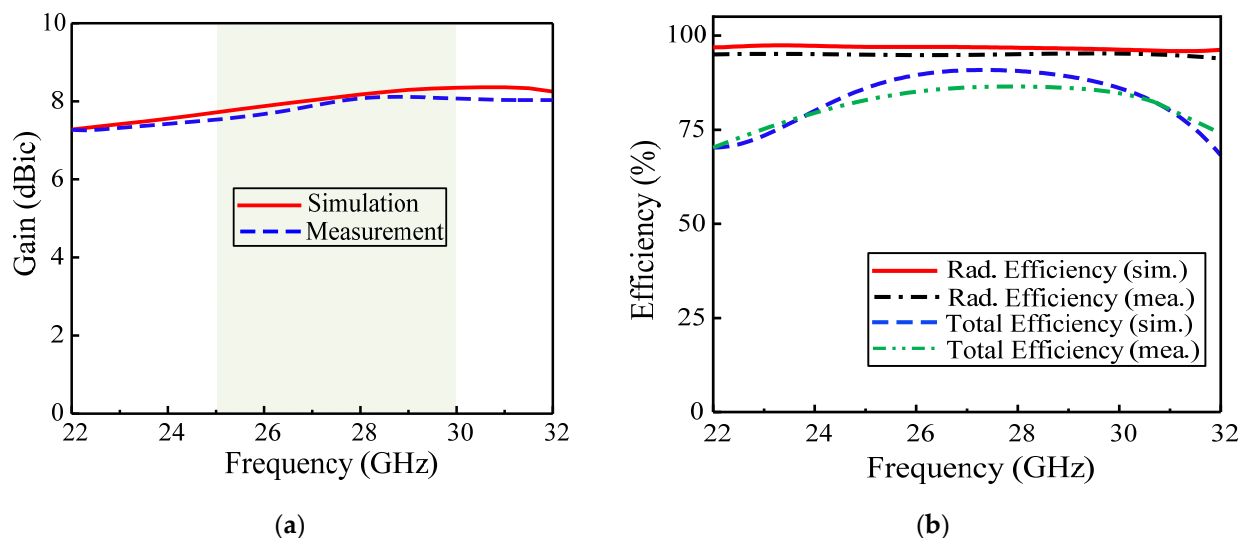


Figure 6. Proposed CP ME dipole antennas: (a) broadside gain, (b) radiation efficiency and total efficiency.

3.3. Radiation Patterns

The measured and simulated radiation patterns of the proposed antenna are shown in Figure 7. The radiations patterns were analyzed in both the xz - and yz -principal planes for 28.5 GHz and 29.5 GHz frequencies. Since the LHCP radiations were minor, the antenna had stable RHCP radiation patterns. At 28.5 GHz, the antenna showed a gain of 8.2 dBic, a front to

back ratio of 26.9 dB, and an angular beamwidth (3 dB) of 61.1 and 74.3 in xz - and yz -planes, respectively. At 29.5 GHz, the antenna showed a gain of 8.3 dBic, a front to back ratio of 26.7 dB, and angular beamwidth (3 dB) of 58 and 76.5 in xz - and yz - planes, respectively.

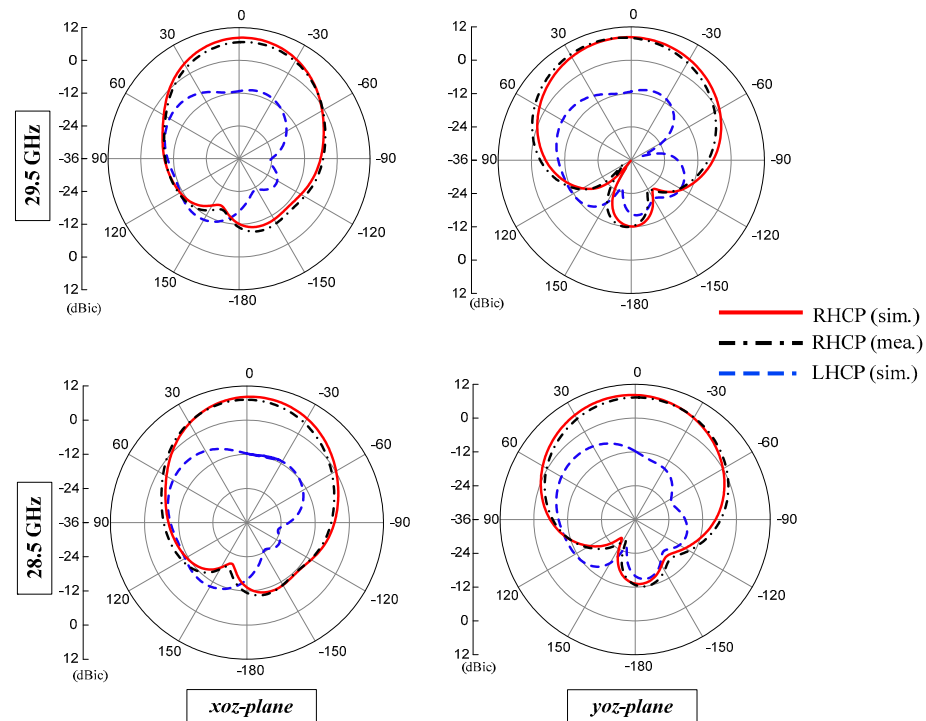


Figure 7. Radiation patterns of the proposed CP ME dipole antenna for different frequencies.

3.4. Performance Comparison

Table 2 shows the comparison of the proposed antenna with the similar state-of-the-art CP ME dipole antennas. To ensure a fair comparison, different performance metrics including antenna design geometry, antenna volume, frequency of operation, polarization, AR bandwidths, and the peak gain value are considered. It can be seen from the table that the proposed antenna demonstrated outstanding performance in terms of overall size, AR bandwidth, and peak gain. Many interesting designs of CP antennas based on ME dipole structure have been reported [8,16–25]. The proposed antenna is the smallest among its competitors with comparable gain and CP bandwidth. The antennas presented in [8,16] have smaller gain narrow bandwidth. The antennas presented in [17–19] have superiority in terms of bandwidth at the expense of larger antenna size, although, their gain performance is comparable with our proposed antenna. The antenna design in [20] has the advantages of higher gain (10.4 dBi), however, it has the limitations of narrower bandwidth and larger antenna profile. Similarly, the mm-wave ME CP antenna in [21] has the merits of wide bandwidth but has lower gain and a larger size. Although the design developed in [22] offers a very wide AR bandwidth due to its novel feeding mechanism, it has limited gain and 3D geometry with a high antenna profile. The CP ME antenna arrays offer wideband and high gain due to their increased number of radiating elements, which, of course, increases the antenna size and complex feeding networks [23–25]. It is noted that our antenna consists of a single element and has a stable gain (average 8 dBic) with a deviation of only ± 0.5 dBic. In conclusion, the proposed antenna outperforms the existing CP ME dipole antennas with its highest gain of 8.5 dBic, wide 3 dB AR bandwidth (18.1%), and a small volume of only $0.83 \lambda_0 \times 0.83 \lambda_0 \times 0.125 \lambda_0$. Since MIMO antennas with increased gain are the key requirements for the 5G systems [32], this work can be extended for MIMO configuration with enhanced isolation in the future.

Table 2. Performance comparison of the proposed CP ME dipole antenna with the reported works.

Ref.	Antenna Type	Antenna Volume (λ_0^3)	f_c (GHz)	Polarization	3 dB ARBW (%)	Peak Gain (dBic)
[8]	ME dipole antenna	$1.54 \times 0.48 \times 0.291$	29	CP	4.8	5.1
[16]	ME dipole antenna	$1.18 \times 1.05 \times 0.122$	24	CP	12.8	7.8
[17]	ME dipole antenna	$1.6 \times 1.3 \times 0.26$	2.5	CP	71.5	8
[18]	ME dipole antenna	$1.1 \times 1.1 \times 0.29$	2.2	CP	47.7	8.6
[19]	ME dipole antenna	$6 \times 6 \times 0.305$	60	CP	23.4	8.6
[20]	ME dipole antenna	$1.12 \times 3.03 \times 0.6$	60	CP	11.6	10.4
[21]	ME dipole antenna	$1 \times 1 \times 0.315$	60	CP	21.9	7.9
[22]	ME dipole antenna	$0.85 \times 0.85 \times 0.18$	2.3	CP	53.2	6.6
[23]	ME dipole antenna array	Not given	28.8	CP	9.7	7
[24]	ME dipole antenna array	Not given	35.2	CP	44	19.2
[25]	ME dipole antenna array	Not given	27	CP	27.8	20.2
This work	ME dipole antenna	$0.83 \times 0.83 \times 0.125$	28	CP	18.1	8.5

4. Conclusions

An ME dipole antenna with RHCP radiation for unidirectional radiation characteristics is characterized and achieved for 5G mm-wave communication systems. The proposed antenna comprises two pairs of rotational symmetric electric dipoles and two pairs of metallic vias perpendicular to the ground plane, acting as a magnetic dipole. An L-shape probe is used to excite the antenna. Owing to the shape of the electric dipoles together with the complementary effect, it produces CP radiations. This antenna has impedance bandwidth of 24.6 for $|S_{11}| < -10$ dB and 3 dB AR bandwidth of 18.1%. The antenna has achieved a peak gain of 8.5 dBic with a compact overall size of $0.83 \lambda_0 \times 0.83 \lambda_0 \times 0.125 \lambda_0$. The wide CP bandwidth, stable radiation characteristics, high efficiency, and low profile of the proposed antenna makes it a suitable candidate for 5G smart devices and sensors.

Author Contributions: Conceptualization, N.H. and H.A.; methodology, H.A. and M.A.S.; validation, S.M.L.; formal analysis, N.H. and H.A.; investigation, H.A. and M.A.S.; writing—original draft preparation, H.A. and N.H.; writing—review and editing, N.H. and H.A.; supervision, N.K.; project administration, N.K. All authors have read and agreed to the published version of the manuscript.

Funding: This work was supported in part by Institute for Information and Communication Technology Promotion (IITP) (A Study on Public Health and Safety in a Complex EMF Environment), under grant 2019-0-00102, and in part by Radio Research Agency (RRA) (Development of Rapid Antenna Measurement Technique for Antennas with New Radio Technology).

Institutional Review Board Statement: Not applicable.

Informed Consent Statement: Not applicable.

Data Availability Statement: All data are included in the manuscript.

Acknowledgments: The author acknowledges the research environment provided by OIP Lab, Chungbuk National University, Korea.

Conflicts of Interest: The authors declare no conflict of interest.

References

- Dangi, R.; Lalwani, P.; Choudhary, G.; You, I.; Pau, G. Study and investigation on 5G technology: A systematic review. *Sensors* **2022**, *22*, 26. [[CrossRef](#)] [[PubMed](#)]
- 5G Frequency Bands. Available online: <https://halberdbastion.com/technology/cellular/5g-nr/5g-frequency-bands/n257-28-ghz> (accessed on 5 January 2022).
- Nalanagula, R.; Darimireddy, N.K.; Kumari, R.; Park, C.-W.; Reddy, R.R. Circularly polarized hybrid dielectric resonator antennas: A brief review and perspective analysis. *Sensors* **2021**, *21*, 4100. [[CrossRef](#)] [[PubMed](#)]
- Sabban, A. Wearable circular polarized antennas for health care, 5G, energy harvesting, and IoT systems. *Electronics* **2022**, *11*, 427. [[CrossRef](#)]
- Trinh, L.H.; Truong, N.V.; Ferrero, F. Low cost circularly polarized antenna for IoT space applications. *Electronics* **2020**, *9*, 1564. [[CrossRef](#)]
- Nguyen, H.Q.; Le, M.T. Multiband ambient RF energy harvester with high gain wideband circularly polarized antenna toward self-powered wireless sensors. *Sensors* **2021**, *21*, 7411. [[CrossRef](#)]

7. Hussain, N.; Jeong, M.; Park, J.; Kim, N. A Broadband circularly polarized Fabry-Perot resonant antenna using a single-layered PRS for 5G MIMO applications. *IEEE Access* **2019**, *7*, 42897–42907. [[CrossRef](#)]
8. Zhang, C.; Chen, H. A broadband circularly polarized substrate integrated antenna with dual magnetoelectric dipoles coupled by crossing elliptical slots. In Proceedings of the 2018 IEEE 18th International Conference on Communication Technology (ICCT), Chongqing, China, 8–11 October 2018; pp. 564–567.
9. Nkimbeng, C.H.; Wang, H.; Park, I. Coplanar waveguide-fed bidirectional same-sense circularly polarized metasurface-based antenna. *J. Electromagn. Eng. Sci.* **2021**, *21*, 210–217. [[CrossRef](#)]
10. Zambak, M.F.; Yasin, M.N.M.; Adam, I.; Iqbal, J.; Osman, M.N. Higher-order-mode triple band circularly polarized rectangular dielectric resonator antenna. *Appl. Sci.* **2021**, *11*, 3493. [[CrossRef](#)]
11. Luk, K.M.; Wong, H. A new wideband unidirectional antenna element. *Int. J. Microw. Opt. Technol.* **2006**, *1*, 35–44.
12. Tan, W.; Xiao, Y.; Li, C.; Zhu, K.; Luo, H.; Sun, H. A wide-band high-efficiency hybrid-feed antenna array for mm-Wave wireless systems. *Electronics* **2021**, *10*, 2383. [[CrossRef](#)]
13. Wang, Y.; Tan, W.; Zhu, K.; Luo, H.; Zhao, G.; Sun, H. Design of A Ka-band 3D-printed dual-polarization magnetoelectric dipole antenna array with low sidelobe. *Electronics* **2021**, *10*, 2969. [[CrossRef](#)]
14. Mak, K.M.; Luk, K.M. A circularly polarized antenna with wide axial ratio beamwidth. *IEEE Trans. Antennas Propag.* **2009**, *57*, 3309–3312.
15. Ta, S.X.; Park, I. Crossed dipole loaded with magneto-electric dipole for wideband and wide-beam circularly polarized radiation. *IEEE Antennas Wirel. Propag. Lett.* **2014**, *14*, 358–361. [[CrossRef](#)]
16. Wu, S.; Zhao, J.; Xu, J. A circularly polarized low-profile magnetoelectric dipole antenna. *Microw. Opt. Technol. Lett.* **2021**, *63*, 2852–2858. [[CrossRef](#)]
17. Kang, K.; Shi, Y.; Liang, C.-H. A wideband circularly polarized magnetoelectric dipole antenna. *IEEE Antennas Wirel. Propag. Lett.* **2017**, *16*, 1647–1650. [[CrossRef](#)]
18. Li, M.; Luk, K.-M. A wideband circularly polarized antenna for microwave and millimeter-wave applications. *IEEE Trans. Antennas Propag.* **2014**, *62*, 1872–1879. [[CrossRef](#)]
19. Ruan, X.; Qu, S.-W.; Zhu, Q.; Ng, K.B.; Chan, C.H. A complementary circularly polarized antenna for 60-GHz applications. *IEEE Antennas Wirel. Propag. Lett.* **2016**, *16*, 1373–1376. [[CrossRef](#)]
20. Bai, X.; Qu, S.-W.; Yang, S.; Hu, J.; Nie, Z.-P. Millimeter-wave circularly polarized tapered-elliptical cavity antenna with wide axial-ratio beamwidth. *IEEE Trans. Antennas Propag.* **2015**, *64*, 811–814. [[CrossRef](#)]
21. Zhu, Q.; Ng, K.-B.; Chan, C.H. Printed circularly polarized spiral antenna array for millimeter-wave applications. *IEEE Trans. Antennas Propag.* **2016**, *65*, 636–643. [[CrossRef](#)]
22. Ding, X.; Wu, S.; Yang, G.; Lan, H. Dual Circularly polarized wideband magneto-electric dipole antenna for wireless applications. *Prog. Electromagn. Res. Lett.* **2022**, *102*, 27–36. [[CrossRef](#)]
23. Wang, Y.F.; Wu, B.; Zhang, N.; Zhao, Y.T.; Su, T. Wideband circularly polarized magneto-electric dipole 1x2 antenna array for millimeter-wave applications. *IEEE Access* **2020**, *8*, 27516–27523. [[CrossRef](#)]
24. Xiang, L.; Wu, F.; Yu, C.; Jiang, Z.H.; Yao, Y.; Hong, W. A wideband circularly polarized magneto-electric dipole antenna array for millimeter-wave applications. *IEEE Trans. Antennas Propagation.* **2021**. [[CrossRef](#)]
25. Feng, B.; Lai, J.; Chung, K.L.; Chen, T.Y.; Liu, Y. A compact wideband circularly polarized magneto-electric dipole antenna array for 5G millimeter-wave application. *IEEE Trans. Antennas Propag.* **2020**, *68*, 6838–6843. [[CrossRef](#)]
26. Causse, A.; Rodriguez, K.; Bernard, L.; Sharaiha, A.; Collardey, S. Compact bandwidth enhanced cavity-backed magneto-electric dipole antenna with outer G-shaped probe for GNSS bands. *Sensors* **2021**, *21*, 3599. [[CrossRef](#)]
27. Hussain, N.; Jeong, M.; Abbas, A.; Kim, N. Metasurface-based single-layer wideband circularly polarized MIMO antenna for 5G millimeter-wave systems. *IEEE Access* **2020**, *8*, 130293–130304. [[CrossRef](#)]
28. Hussain, N.; Jeong, M.; Abbas, A.; Kim, T.; Kim, N. A metasurface-based low-profile wideband circularly polarized patch antenna for 5G millimeter-wave systems. *IEEE Access* **2020**, *8*, 22127–22135. [[CrossRef](#)]
29. Li, R.-L.; Fusco, V.F.; Nakano, H. Circularly polarized open-loop antenna. *IEEE Trans. Antennas Propag.* **2003**, *51*, 2475–2477.
30. Askari, H.; Hussain, N.; Domin Choi, M.; Sufian, A.; Abbas, A.; Kim, N. An AMC-based circularly polarized antenna for 5G sub-6 GHz communications. *CMC-Comput. Mater. Contin.* **2021**, *69*, 2997–3013. [[CrossRef](#)]
31. Lim, J.H.; Lee, J.W.; Lee, T.K. Cross-pol pattern effects of parabolic reflector antennas on the performance of spaceborne quad-pol SAR systems. *J. Electromagn. Eng. Sci.* **2021**, *21*, 218–227. [[CrossRef](#)]
32. Lavdas, S.; Gkonis, P.K.; Zinonos, Z.; Trakadas, P.; Sarakis, L. An adaptive hybrid beamforming approach for 5G-MIMO mmWave wireless cellular networks. *IEEE Access* **2021**, *9*, 127767–127778. [[CrossRef](#)]